JOURNAL OF MATERIALS SCIENCE 31 (1996) 5257–5270

Rheological properties of Al_2O_3–SiC whisker composite suspensions

L. BERGSTRÖM
Institute for Surface Chemistry, P.O. Box 5607, S-114 86 Stockholm, Sweden

The rheological properties of both aqueous and non-aqueous composite suspensions were investigated together with a characterization of the colloidal stability of the separate components. The colloidally stable, concentrated aqueous SiC_w and Al_2O_3–SiC_w composite suspensions displayed strong shear thinning followed by a severe, sometimes discontinuous, shear thickening at a critical shear rate. The non-aqueous composite suspensions, containing weakly flocculated SiC_w, only showed a continuous shear thinning behaviour. The variations in the steady shear behaviour were related to the differences in the colloidal stability and possible shear induced effects on the suspension structure. It was possible to fit the volume fraction dependence of both the SiC_w and the Al_2O_3 suspensions to a modified Krieger–Dougherty model which yields values of the maximum volume fraction; ϕ_m (Al_2O_3) = 0.61, ϕ_m(SiC_w) = 0.28. The viscosity of the composite suspensions were successfully predicted from the Farris theory using the rheological data for the separate components.

1. Introduction

Ceramics are brittle materials with a tendency to catastrophic failure. This inherent problem has motivated many researchers to explore different approaches to improve the strength and reliability. Based on the Griffith relation [1], these approaches are either focused on increasing the fracture toughness or decreasing the size of the largest flaws. Flaw minimization through process optimization can be successfully accomplished by colloidal processing, which involves the manipulation and control of interparticle forces in powder suspensions in order to remove heterogeneities and to optimize suspension properties [2–4]. The fracture toughness of ceramics can be improved by the incorporation of reinforcing phases, such as particulates, plateletes and whiskers [5]. For example, the fracture toughness can be improved two to three times by incorporating SiC whiskers into a ceramic matrix [6].

Unfortunately, the incorporation of whiskers into a powder body does present problems of both a processing and densification nature. With a significant amount (> 10 vol %) of whiskers present, complete densification is usually only achieved if an external pressure is applied, e.g. by hot pressing [6, 7]. Mixing of components and the forming of a green body with optimal properties also becomes increasingly more difficult with increasing amount of the added anisotropically shaped whiskers. It is essential to obtain a good dispersion of the whiskers in the particulate matrix to achieve high densities and optimum mechanical properties of the sintered detail. It was early recognized that the presence of fibre bundles and a non-uniform distribution of the whiskers will limit the fracture strength of composites [8, 9]. These processing problems are in conflict with the early observation that the fracture toughness increases with increasing amount of whiskers [6].

In order to achieve a homogeneous mixing of whiskers and particles and to break up whiskers bundles, the components are often dispersed and mixed in a continuous medium before shape forming [10]. The continuous medium can either be a low molecular weight liquid or a high molecular weight polymer. While hot-pressing, the most commonly used forming method for composites, produces dense materials, this method is limited to the fabrication of simple shapes. Hence, it is of interest to use other types of forming methods, such as slip casting, pressure filtration and injection moulding which can produce complicated bodies of near net-shape. Slip casting or pressure filtration in water have been used to produce green bodies of Si_3N_4/SiC_w [11], Al_2O_3/Si_3N_{4w} [12], and Al_2O_3/SiC_w [7, 13] composites. Si/SiC_w composite green bodies were formed by extrusion in a polymer wax [14].

During forming, the concentrated composite suspension is subjected to an applied stress to form it into an engineering shape. In all types of suspension shape forming techniques, ranging from slip casting to injection moulding, the rheological properties of the concentrated suspension play a key role in controlling the shape-forming behaviour and optimizing the properties of the green body. Fundamentally, the rheological properties of concentrated colloidal suspensions are determined by an interplay of thermodynamic and fluid mechanical interactions. This means that there exists an intimate relation

0022–2461

between the particle interactions, including Brownian motion, the suspension structure (i.e. the spatial particle distribution in the liquid) and the rheological response. With particles in the colloidal size range (at least one dimension $< 1\ \mu m$), the range and magnitude of the interparticle forces will have a profound influence on the suspension structure and hence, the rheological behaviour [15, 16]. Both the fluid mechanical interactions and the interparticle forces are strongly dependent on the average separation distance between the suspended particles. Hence, the rheological behaviour of concentrated suspensions is a function of solids concentration and particle size. A generally observed phenomenon is that the viscosity increases with volume fraction of solids and the suspension finally ceases to flow at some critical maximum volume fraction of solids, ϕ_m. It has been found that solid material with a high aspect ratio (fibres) or irregular shape yields a low ϕ_m and higher viscosities than spherical particles [17]. Hence, from fundamental considerations regarding the rheology of concentrated suspensions, it is expected that the incorporation of anisotropic whiskers will greatly affect the rheological properties of composite mixtures.

There are only a few studies published where a more thorough investigation of the rheological properties of concentrated composite suspensions have been reported [18, 19]. Both of these studies were performed with the solid material dispersed into a high-viscosity medium and the rheological measurements were performed by capillary viscometry at high shear rates and shear stresses. Attempts were made to predict the relative viscosities of the composite suspensions as a function of volume fraction of solids and whiskers content using different types of semi-empirical relations. Because these studies focused on the high shear stress behaviour with the application of injection moulding in mind, the effect of the state of dispersion of the components in the liquid polymer at high temperature was not covered in detail. It is generally believed that the interparticle forces play a minor role when a suspension is subjected to high shear stresses or shear rates because the hydrodynamic interactions will dominate and assist in the breakdown of any type of aggregate. However, in low-pressure forming techniques, e.g. slip casting, the shear rates are low and the interparticle forces will dominate the behaviour of concentrated casting suspensions.

In this study, the rheological properties of both aqueous and non-aqueous composite suspensions were investigated. The objective was to characterize the rheological behaviour in detail of both the separate components and the composite mixtures and to elucidate the effect of the amount of dispersant added, the colloidal stability of the suspensions and the volume fraction of solids. This paper is divided into four sections. The first section discusses the characterization and colloidal stability of the powder and whisker in both aqueous and non-aqueous media. The second section demonstrates how rheological measurements can be used to characterize the colloidal stability and optimize the amount of dispersant added. The third section discusses the steady shear behaviour of both the different components and the composite suspensions and relates the behaviour to the colloidal stability of the components and the suspension structure. The fourth section focuses on the effect of volume fraction of solids of both particles, whiskers and composite mixtures on the steady shear viscosity. The experimental results were fitted to a proposed model predicting the volume fraction dependence of the relative viscosity of monomodal and bimodal suspensions.

2. Experimental procedure

2.1. Materials

The alumina powder was A16SG obtained from Alcoa, USA. It is a high purity α-alumina powder consisting of more than 99.9 wt % alumina. The main impurities are sodium (400 p.p.m.), magnesium (100 p.p.m.), iron (70 p.p.m.), calcium (100 p.p.m.) and silicon (90 p.p.m.). The impurities were determined by optical emission spectroscopy using a Hilger E1000 instrument. The silicon carbide whisker was obtained from ACMC, Greer, South Carolina, USA. The whiskers are produced from rice hulls in a graphite furnace [20]. The main impurities are calcium (~ 500 p.p.m.), magnesium (100 p.p.m.) and iron (~ 200 p.p.m.). The whiskers are oxidized with an oxygen content ~ 0.7 wt %.

The particle-size distribution of the alumina powder was measured by a Micromeritics model 5100 Sedigraph instrument. The length and aspect ratio of the silicon carbide whiskers after premilling to reduce the aspect ratio, normally being more than 40 [21], were determined from cursory inspection of scanning electron micrographs. More than 200 whiskers were evaluated. The specific surface area was determined from single-point BET measurements using a Ströhlein instrument.

The aqueous suspensions were prepared using water purified with a Milli-Q system (Millipore Corporation, USA) and an anionic polyelectrolyte Dispex A40 (Allied Colloids, USA) was used as dispersant. The non-aqueous suspensions were prepared using decahydronaphtahlene (decalin) as solvent (99% +, Aldrich Chemicals). This solvent was chosen because of its high purity, non-polar nature and low vapour pressure at room temperature (~ 1 mbar, $\sim 10^2$ Pa). Decalin has a density of 0.896 g cm^{-3}, refractive index of 1.475 and static relative premitivity of 2.1 [22]. The viscosity was measured as 3.0 mPas at 25 °C. The dispersant used for the non-aqueous suspensions was Hypermer KD3, ICI Chemicals, UK with a density of 0.92 g cm^{-3}. The dispersant acts as a steric stabilizer and consists of a multi-functional head group and polyester-type stabilizing moieties [23]. The amounts of Hypermer KD3 and Dispex A40 reported in this paper correspond to pure substance.

Adsorption isotherms of Hypermer KD3 on alumina and silicon carbide whiskers in decalin were determined by potentiometric titrations in non-aqueous media. The electrophoretic mobility of very dilute

(0.1 wt % solids) aqueous suspensions of alumina and silicon carbide whiskers in 0.01 M NaCl electrolyte was measured by the microelectrophoresis technique using a Zeta-sizer MK4, Malvern Instruments, UK. The colloidal stability was qualitatively evaluated by settling rate experiments. Diluted suspension (3 wt %) of silicon carbide whiskers and alumina powders were prepared, poured into graduated tubes and the settling rate was measured.

2.2. Suspension preparation

The alumina powder was always dried in vacuum over phosphorous pentoxide at room temperature overnight before mixing. Decalin was dried over 4A molecular sieves for at least 24 h before use. Dispex A40 was used as a 25 wt % stock solution in water. As-received Hypermer KD3 was dissolved in dry decalin before being added to the non-aqueous suspensions in the form of a concentrated stock solution, in order to improve mixing and facilitate rapid adsorption of the dispersant on the particle surfaces.

The one-component suspensions and composite suspensions at low and intermediate concentrations were prepared by first weighing appropriate amounts of powder and whisker in a beaker and then adding solvent and dispersant. The solid and the liquid were mixed with a spatula and, if the mixture was not too thick, with a magnetic stirrer.

Composite suspensions of high concentration were prepared by first dispersing the alumina powder and then adding the whiskers in portions to facilitate a good mixing and dispersion. All the composite suspensions were prepared at a constant composition Al_2O_3/SiC_w (75/25 wt %) equivalent to 30 vol % SiC_w. After a minimum mixing time of 1 h, the suspensions were treated with an ultrasonic horn of diameter 9.5 mm (Soniprep 150, MSE Scientific Instruments, UK). The samples were treated in 5 min sequences until no agglomerates could be visibly detected. In most cases one or two sequences were sufficient to obtain a well-dispersed sample. Each sample was cooled during ultrasonication by immersion of the beaker in an ice bath. The suspensions were prepared in 25 ml batches to maximize the effect of the ultrasonic treatment.

After ultrasonication, the suspensions were kept in sealed flasks under continous slow stirring for at least 16 h before rheological measurements. This treatment ensured that no air remained in the suspension and that the samples equilibrated after ultrasonication.

2.3. Rheological measurements

The steady-shear and viscoelastic rheological properties were determined using a Bohlin VOR (Bohlin Rheologie, Lund, Sweden) equipment. Measurements were performed with a concentric cylinder measurement geometry, C 25, with a gap between the inner and outer cylinder walls of 1.25 mm. A solvent trap was used to minimize evaporation of the solvent. All measurements were performed at a temperature of 25 °C. Each sample was allowed a maximum time of 3 h in the C25 geometry to minimize the effect of sedimentation.

Steady-shear measurements were performed in the shear-rate range of 0.1–1000 s^{-1} by incrementally changing the shear rate and measuring the shear stress after a determined equilibration time at each shear rate. Measurements were performed by initially stepping up and then stepping down in shear rate. The equilibration time was chosen long enough to allow the suspension to reach steady state. Typical equilibration times ranged from 40–300 s where the equilibration time increases with increasing solids concentration and decreasing shear rate.

Viscoelastic measurements were performed using the same measurement geometry. A sinusoidal strain was applied and the stress and phase shift between the stress and strain was measured. All measurements were performed in the linear viscoelastic region where the viscoelastic response was independent of strain. In this region, the storage modulus, G', and the loss modulus, G'' are directly obtained [24].

3. Results and discussion

3.1. Characterization and dispersion of powder and whisker

A scanning electron micrograph of the silicon carbide whiskers is shown in Fig. 1. Most of the whiskers have a straight cylindrical geometry but it can be seen that some whiskers have stacking faults which render them an irregular shape. The whiskers show a large variation in length, from 1–50 μm with an average length of 5.7 μm. The average diameter is 0.6 μm. The particle-size distribution of the alumina powder is shown in Fig. 2. The powder has a rather broad particle-size distribution with an average particle diameter around 0.4 μm. The powder also contains some larger agglomerates with a size between 5 and 10 μm.

The particle-size data, together with specific surface area, pH of the isoelectric point, pH_{iep}, and the maximum amount of Hypermer KD3 adsorbed from decalin, Γ_M, are shown in Table I. The measured specific surface area of the whiskers, 3.9 $m^2 g^{-1}$, is in acceptable agreement with the surface area calculated from

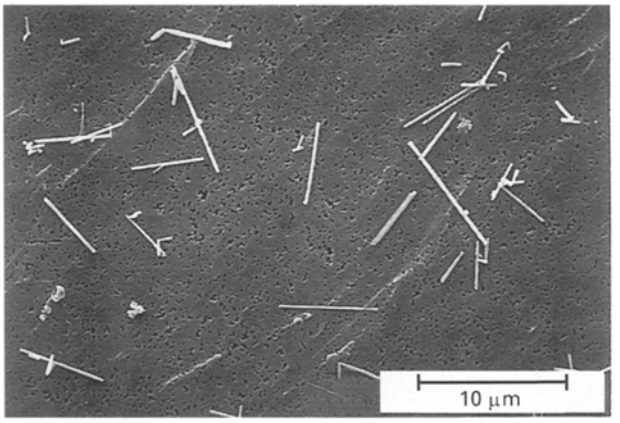

Figure 1 Scanning electron micrograph of the ACMC silicon carbide whiskers. The bars represent 10 μm.

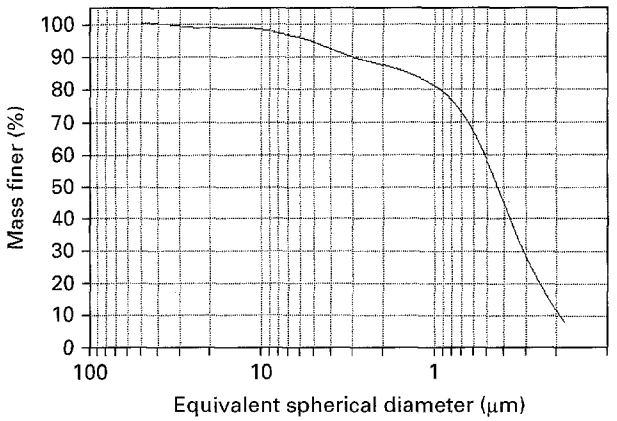

Figure 2 Cumulative mass particle-size distribution of alumina powder A16SG.

TABLE I Characteristics of alumina powder and silicon carbide whisker

	Al_2O_3 powder	SiC whisker
Specific surface area ($m^2 g^{-1}$)	8.0	3.9
Median particle diameter (μm)	0.4	
Average length (μm)		5.7
Average diameter (μm)		0.6
Average aspect ratio		9.5
pH_{iep}	8.8	2
Γ_M of KD3 ($mg m^{-2}$)	10	5

the average length and diameter of the cylindrical whiskers ($2.2 m^2 g^{-1}$) considering the large variation in whisker length. The measured isoelectric points for both alumina ($pH_{iep} = 8.8$) and the silicon carbide whiskers ($pH_{iep} = 2$) agree well with earlier work on the electrokinetic properties of alumina [25, 26] and SiC particles [27, 28]. The adsorption isotherms of Hypermer KD3 on the SiC whiskers and the Al_2O_3 powder was of the high-affinity type with a well-defined plateau at high equilibrium concentrations of KD3 in the solution (decalin). The maximum amount adsorbed ($\Gamma_M(Al_2O_3) = 10 mg m^{-2}$, $\Gamma_M(SiC_w) = 5 mg m^{-2}$) corresponds to ~2 wt % KD3 on SiC_w and ~8 wt % KD3 on Al_2O_3.

Although the colloidal stability and dispersion of the alumina and silicon carbide whiskers in both aqueous and non-aqueous media will be discussed in detail in a forthcoming paper [29], some general features will be described here. The alumina powder and the silicon carbide whiskers were dispersed in decalin, a non-polar solvent, by adding Hypermer KD3. KD3 has been found to be an efficient dispersant in non-polar media for a number of different ceramic powders such as silicon and Al_2O_3 [30] and Si_3N_4 [30, 31]. In aqueous media, the alumina and silicon carbide whiskers were dispersed by the addition of Dispex A40, an anionic polyelectrolyte, at pH ~ 9. Previous studies have shown that anionic polyelectrolytes of low molecular weights are efficient dispersants for alumina at pH ~ 9 [32]. Measurements of the electrophoretic mobility showed that the pH_{iep} of alumina shifted from $pH_{iep} = 8.8$ to $pH_{iep} = 4$ when Dispex A40 was added [29]. Hence, both the alumina powder and the silicon carbide whiskers will have a large negative surface charge at pH ~ 9 with Dispex A40 added.

Simple settling-rate experiments of dilute suspensions showed that the alumina powder was colloidally stable in both the non-aqueous and aqueous media with the added dispersants, Hypermer KD3 and Dispex A40, respectively. The particles settled very slowly and a cloudy supernatant layer was formed after several days of settling. This is typical for the settling of a well dispersed suspension with a broad particle size distribution. Each particle settles as an individual unit and because the small particles have a much slower settling rate, they remain in the supernatant. The silicon carbide whisker aqueous suspension, dispersed at pH ~ 9 with 0.25 wt % Dispex A40 added, showed the same type of slow settling with the formation of a cloudy supernatant, indicating that the aqueous whiskers suspension is also colloidally stable. The non-aqueous whisker suspension with the whiskers dispersed in decalin with 2 wt % KD3 added, displayed rapid settling with the formation of a dense sediment after less than 2 h. This shows that the whiskers are flocculated with the formation of large aggregates which settle rapidly.

This difference in the behaviour of the aqueous and non-aqueous whiskers suspensions can be related to the difference in range and magnitude of the repulsive interaction. The surface charge on the whisker surface in an aqueous medium will create a strong repulsive interaction through the formation of an electrical double layer [33]. At a sufficiently low ionic strength, the repulsion will be long range and thus create a colloidally stable suspension. The magnitude and range of the steric repulsion created by an adsorbed polymer layer like Hypermer KD3, is determined by a number of factors, such as the solvent condition, strength of adsorption, layer density and thickness [34]. It is currently believed that the polymeric dispersant used, Hypermer KD3, creates a sufficiently thick layer to screen the van der Waals forces for the small alumina particles but not for the larger silicon carbide whiskers [29]. This results in a weak flocculation of the non-aqueous silicon carbide whiskers suspensions. Table II summarizes the colloidal stability of the separate components in both aqueous and non-aqueous media. More details on the colloidal stability including calculations of the interparticle energies for these systems will be presented in a forth coming paper [29].

TABLE II The colloidal stability of alumina particles and silicon carbide whiskers with an anionic polyelectrolyte, Dispex A40 and a block copolymer, Hypermer KD3 added to the aqueous and non-aqueous suspensions

	Dispersion medium/dispersant	
Solid phase	Water/Dispex A40	Decalin/KD3
Al_2O_3 particles	Dispersed	Dispersed
SiC_w	Dispersed	Flocculated

3.2. Optimization of the amount of dispersant

Upon the close approach of two particles covered with adsorbed polymer layers, the interpenetration of the polymer layers might give rise to a repulsive force, so called steric stabilization. Any theory trying to describe the magnitude and range of the interaction between polymer layers needs to account for both the solution properties of the polymer and the conformations of the polymer at the solid–liquid interface [34]. This is no simple task and the more realistic theories tend to be rather complicated mathematically. However, in spite of the theoretical complications, it has been possible to state some simple requirements for steric stabilization of colloidal suspensions [34, 35].

(i) The adsorbed polymer layer should be thick enough to prevent the particles from coming into close contact where the van der Waals force will give rise to a net attraction.

(ii) The adsorbed polymer layer should completely cover the particles and be as dense as possible. If the coverage is incomplete or the layer density is too low, the particles may come into close contact. Bridging flocculation might also occur if the coverage is incomplete.

(iii) The polymer should be firmly "anchored" to the surface of the particle. If the adsorption is too weak, the polymer may desorb during a particle collision.

(iv) The stabilizing moieties should be in a good solvent condition. If the solvent condition is bad, interaction between two polymer layers will result in an attractive, and not a repulsive force.

Because Hypermer KD3 adsorbs strongly on the alumina and silicon carbide surfaces and because decalin is a good solvent for the essentially non-polar stabilizing part of the molecule, requirements (iii) and (iv) are fulfilled. Requirements (i) and (ii), on the other hand, can be in conflict with the general goal of maximizing the solids loading in ceramic processing. Although a thick and dense polymer layer is beneficial for the colloidal stability, this layer might occupy a substantial volume and thus lower the volume fraction of the ceramic material in the suspension and subsequently in the green body. Hence, the dispersant added should be optimized to create an effective steric stabilization but occupy a minimum volume. This can be achieved by either varying the molecular weight of the dispersant (which affects the layer thickness) or the total amount adsorbed (which affects both the layer thickness and density). In this study, only the effect of the amount added was investigated.

Fig. 3 shows the steady shear viscosity of concentrated alumina suspensions at constant volume fraction of solids as a function of shear rate and amount of KD3 added. All of these suspensions display a shear thinning behaviour with a drop of at least one order of magnitude of the viscosity from low shear rate ($\dot{\gamma} = 1.5\ s^{-1}$) to high shear rate (the high shear rate plateau) as illustrated in Fig. 3a. The degree of shear thinning (evaluated from the difference between the high and low shear rate viscosity in Fig. 3b) appears to be constant when more than 4 wt % KD3 is added but increases rapidly at additions below 2.5 wt % KD3.

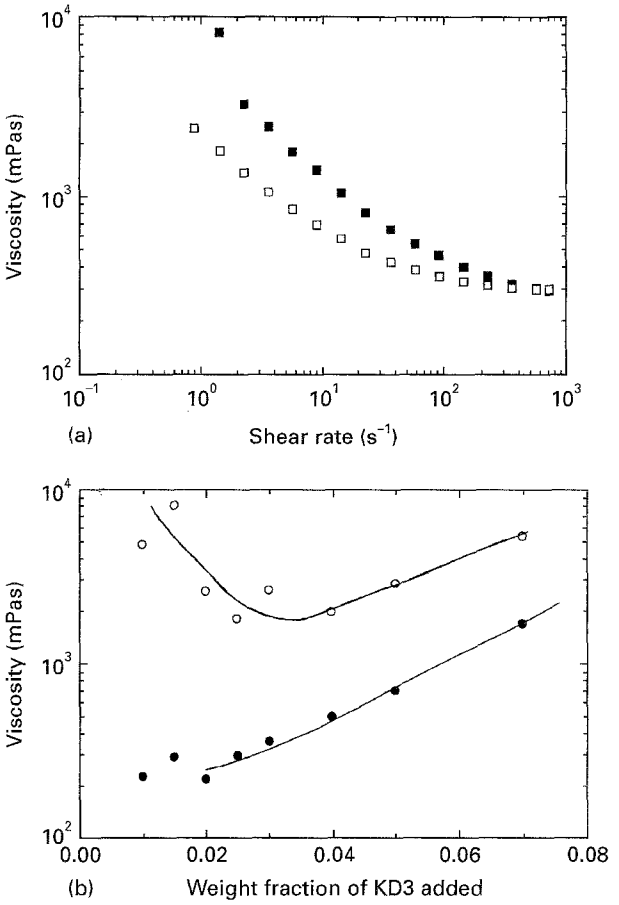

Figure 3 Viscosity of 50 vol % alumina suspensions in decalin, (a) as a function of shear rate, (■) 1.5 wt % KD3 and (□) 2.5 wt % KD3 added, and (b) as a function of amount of Hypermer KD3 added. (b) (●) The viscosities at the high shear rate plateau, (○) the viscosities at a shear rate of $\dot{\gamma} = 1.5\ s^{-1}$.

This change in the degree of shear thinning can be related to a change of the colloidal stability.

Concentrated colloidally stable suspensions display a shear thinning behaviour because of a perturbation of the suspension structure by shear [36]. At low shear rates, the suspension structure is close to the equilibrium structure at rest because thermal motion dominates over the viscous forces. At higher shear rates, the viscous forces affect the suspension structure more, and shear thinning occurs. At very high shear rates, the viscous forces dominate and the plateau in viscosity in this region is a measure of the resistance to flow of a suspension with a completely hydrodynamically controlled structure. Several studies on hard sphere suspensions have shown that shear thinning at high shear rates is associated with some type of induced ordering of the suspension structure [37, 38].

With the particle interactions being dominated by attraction, the severe shear thinning of flocculated suspensions can be explained by the breakdown of aggregates formed. With increasing shear rate, the viscous forces tend to reduce the size of the aggregates and release liquid immobilized in the aggregates, hence facilitating flow [39]. The shear thinning can be reversible or irreversible depending on the degree of flocculation [15]. It has been demonstrated that a concentrated suspension becomes more and more

severely shear thinning with an increase in the magnitude of the interparticle attraction (degree of flocculation) [40]. Hence, the increasing degree of shear thinning at KD3 additions below 2.5 wt % indicates that the alumina suspension starts to become colloidally unstable (Fig. 3). Above 4 wt % KD3 added, the suspension appears to be colloidally stable with a constant degree of shear thinning.

Viscoelastic measurements were also performed to obtain more information regarding the effect of the added amount KD3 on the colloidal stability. Compared to steady-shear measurements, oscillatory viscoelastic measurements are made under small deformations, which means that the structure is only slightly perturbed from the structure at rest. Hence, oscillatory measurements are suitable for correlating rheological data to interparticle forces because the hydrodynamic interactions are minimal. Fig. 4 shows the difference in viscoelastic behaviour of an alumina suspension with 1 and 2.5 wt % KD3 added. The suspension with 2.5 wt % KD3 added shows a viscoelastic behaviour with the viscous (represented by the loss modulus, G'') and the elastic (represented by the storage modulus, G') response of the same magnitude. Both the G' and G'' increase with frequency. The suspension with only 1 wt % KD3 added displays a much stronger elastic behaviour with the storage modulus several times larger than the loss modulus. The weak dependence of G' on frequency indicates that the relaxation time of this suspension is considerably larger than for the suspension with 2.5 wt % KD3 added. A rough estimate of the relaxation time can be obtained from the cross-over point of G' and G''. The elastic behaviour and long relaxation time of the suspension with 1 wt % KD3 added is indicative of formation of a continuous three-dimensional particle network caused by interparticle attraction (flocculation) [41, 42].

Oscillatory measurements were performed on a number of suspensions with different amounts of KD3 added. Fig. 5 shows how the linearity limit and the phase angle at a frequency of 1 Hz varies with the amount of KD3 added. The linearity limit is assessed from strain sweep measurements in which the strain is

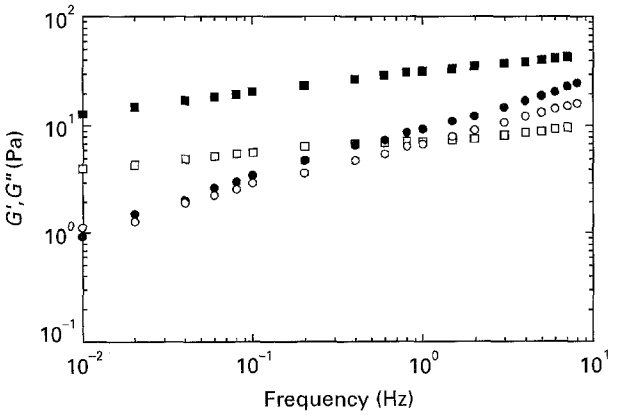

Figure 4 Oscillatory measurements of 50 vol % alumina suspensions in decalin with (■, □) 1 wt % KD3, and (●, ○) 2.5 wt % KD3 added. (■, ●) Storage modulus, G' (□, ○) loss modulus, G''.

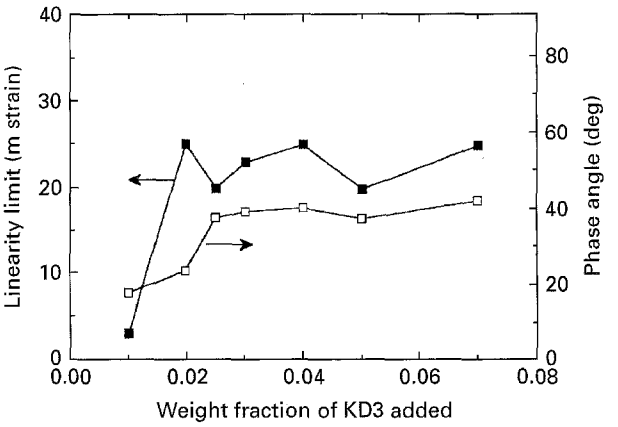

Figure 5 Linearity limit and phase angle obtained from viscoelastic measurements on 50 vol % alumina suspensions in decalin with varying amount of KD3 added. Both the phase angle and the linearity limit measurements were done at a frequency of 1 Hz.

increased and the storage and loss moduli are measured. At low deformations (strain), the viscoelastic response is independent of strain. The limit of this linear viscoelastic region can be defined as the deformation at which the storage modulus starts to decrease. The linearity limit is very low for the suspension with 1 wt % KD3 added but attains a constant value around 20–25 milli strain at KD3 additions above 2 wt %. This behaviour is considered to be related to the transition from a flocculated to a colloidally stable suspension. Three-dimensional particle networks created by attractive interparticle forces are usually more fragile than the liquid-like structure of colloidally stable suspensions. This difference should be manifested in the linearity limit. At deformations above the linearity limit, the particle network starts to break down which results in a lowering of the elastic response. A more flexible particle structure will display a higher linearity limit.

The phase angle, δ, is defined as

$$\tan \delta = G''/G' \quad (1)$$

Hence, a high phase angle means that the material is predominantly viscous while a low phase angle represents an elastic material. Fig. 5 shows that the phase angle is low for low amounts of KD3 added and attains a constant value, $\delta \sim 40°$ at additions above 2.5 wt % KD3. Following the discussion of the oscillatory measurements, this change in phase angle can also be explained by a transition from a flocculated, predominantly elastic suspension to a colloidally stable suspension characterized by a viscoelastic response at these high solids concentrations.

Hence, both the steady-shear measurements in Fig. 4 and the viscoelastic results in Figs 4 and 5 show that a minimum amount of 2.5–3 wt % KD3 is needed to obtain a colloidally stable alumina suspension in decalin. This minimum amount is substantially lower than the maximum adsorbed amount of KD3 (~ 8 wt %). Thus, the results show that an efficient steric repulsion can be created at a rather low polymer surface coverage. It should be stressed that it is

necessary to perform a thorough rheological characterization to obtain relevant information for such an assessment. Fig. 3 clearly shows that a measurement of the viscosity at relatively high shear rate versus the amount of dispersant added might be misleading. Only steady shear measurements at low shear rates or viscoelastic measurements will be dominated by the interparticle forces and hence the state of dispersion.

However, the high shear results in Fig. 3 show that in the colloidally stable region (above 2.5 wt % KD3 added), the viscosity continuously increases with an increase in KD3 added. The increase is quite substantial, from ~300 mPas at 2.5 wt % KD3 added, to ~1800 mPas at 7 wt % KD3 added. Because the volume fraction of solids is kept constant at $\phi = 0.50$, an increase in the amount of KD3 added corresponds to a decrease in the amount of solvent (decalin) added. Practically all of the dispersant added will adsorb on the powder surface and not be available as a continuous, liquid phase. In order to explain the effect of attached polymer layers on the rheological behaviour of concentrated suspensions, other researchers [43, 44] have successfully used the concept of an effective volume fraction, ϕ_{eff}, defined as

$$\phi_{eff} = \phi(1 + \Delta/a)^3 \quad (2)$$

where Δ is the thickness of the polymer layer, a is the radius of the spherical particle and ϕ is the volume fraction of solids. Hence, a thick polymer layer will increase the effective volume fraction substantially. Fig. 6 is an attempt to estimate the effect of the varying amounts of KD3 added by using a modified effective volume fraction estimation. Because the solid alumina particles are polydisperse and non-spherical, Equation 2 cannot be used. Instead, the effective volume fraction of the particles was estimated by assuming a completely dense layer of polymer being formed on the particles, which can be expressed as

$$\phi_{eff} = (V_{solid} + V_{polymer})/V_{total} \quad (3)$$

where V_{solid} and $V_{polymer}$ denote the volume of the respective phases. This is equivalent to assuming that

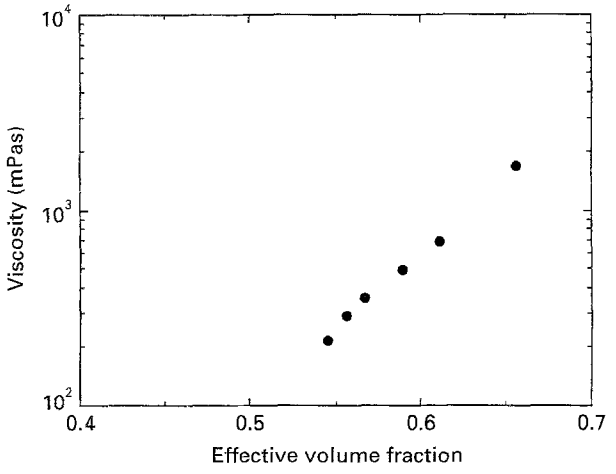

Figure 6 High shear viscosity versus effective volume fraction for colloidally stable non-aqueous alumina suspensions with varying amounts of KD3 added. The effective volume fraction was calculated by assuming a completely dense polymer layer, Equation 3.

the polymer layer thickness is directly related to the amount of dispersant added, because the surface coverage is assumed to be constant (equal to 1). For the suspension with the highest amount of KD3 added (7 wt %) this is equivalent to an effective volume fraction at 65.6 vol %. The result of this calculation can be seen in Fig. 7 where an exponential relation

$$\eta \sim \exp(\phi_{eff}) \quad (4)$$

between the effective volume fraction and high shear viscosity is obtained. This is clearly an unphysical result because all the relations between volume fraction and viscosity predict a diverging increase of the viscosity at some critical volume fraction. These relations will be discussed in detail in Section 3.4. Probably, the inability of fitting the points in Fig. 7 to a suitable model is due to the problem of estimating the effective volume fraction. At low amounts of KD3 added, the polymer layer density (or the surface coverage) will probably be rather low and thus immobilize some of the solvent. At the high amounts of KD3 added, the polymer layer density is probably high and the assumptions made in Equation 3 are then more valid. Hence, the polymer layer thickness, which is the critical parameter in these calculations, is probably only a weak function of the amount of KD3 added. However, it is difficult to use a more sophisticated model until data correlating adsorbed amount of polymer to layer thickness is available. Such measurements, using the surface force technique, are currently being performed.

For the following rheological measurements, an addition of 4.5 wt % KD3 was used to prepare the alumina suspensions in decalin. This somewhat high amount was chosen to ensure colloidal stability. An addition of 2 wt % KD3 was used for the silicon carbide whiskers suspensions in decalin. This amount corresponds to the maximum amount of KD3 being adsorbed on the SiC_w surface. The KD3 addition to the composite suspensions was estimated from the composition of the suspension and the amount KD3 added to each component. This resulted in an addition of 3.9 wt % KD3 to the composite suspensions containing 25 wt % SiC_w. Steady-shear measurements on concentrated composite suspensions at constant solids concentration confirmed that this amount of KD3 added corresponds to the low viscosity region.

The amount of anionic polyelectrolyte, Dispex A40, added to a concentrated aqueous composite suspension was optimized through steady shear measurements at high and low shear rates (Fig. 7). The results show a distinct minimum in the viscosity curves at both low and high shear rates. The results indicate that additions above 0.2 wt % Dispex A40 will result in a colloidally stable suspension. An addition of 0.25 wt % Dispex A40 at pH ~ 9 was used in preparing stable aqueous suspensions of the separate components as well as of the composite mixture.

3.3. Steady-shear rheology

Fig. 8 shows the steady shear viscosity of non-aqueous alumina suspensions at various volume fractions. The

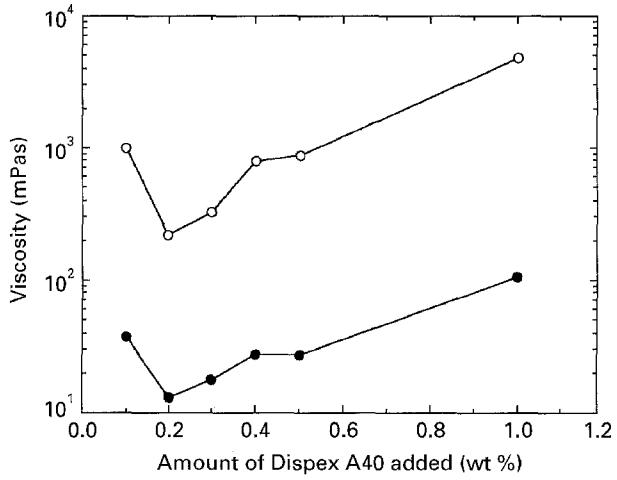

Figure 7 Viscosity of aqueous composite suspensions containing 25 wt % SiC_w at $\phi = 0.35$, plotted as a function of the amount of Dispex A40 added. (●) The high shear rate region ($\dot{\gamma} = 100$ 1/s), (○) the low shear region ($\dot{\gamma} = 1.5\ s^{-1}$).

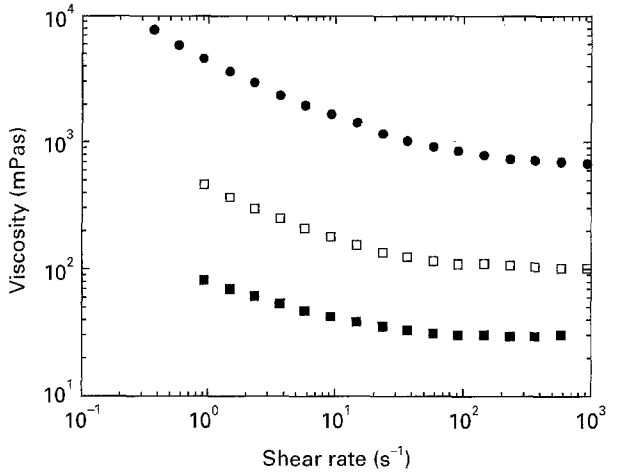

Figure 8 Steady-shear viscosity of alumina suspensions dispersed in decalin with 4.5 wt %. Hypermer KD3 at different volume fractions of solids: ϕ = (■) 0.30, (□) 0.42, (●) 0.50.

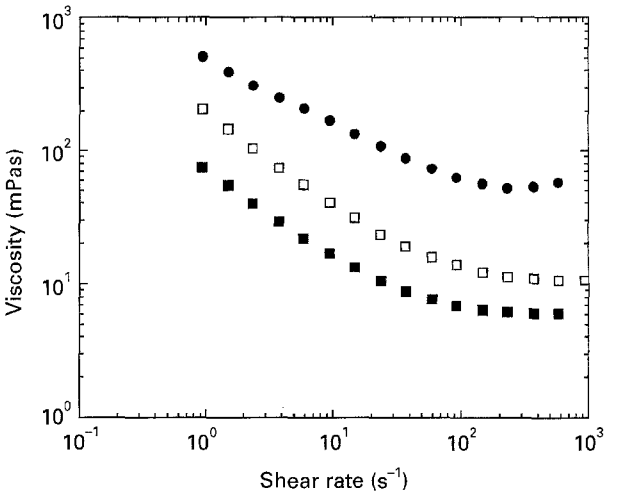

Figure 9 Steady-shear viscosity of silicon carbide whisker suspensions dispersed in decalin with 2 wt % Hypermer KD3 at different volume fractions of solids: ϕ = (■) 0.055, (□) 0.109, (●) 0.180.

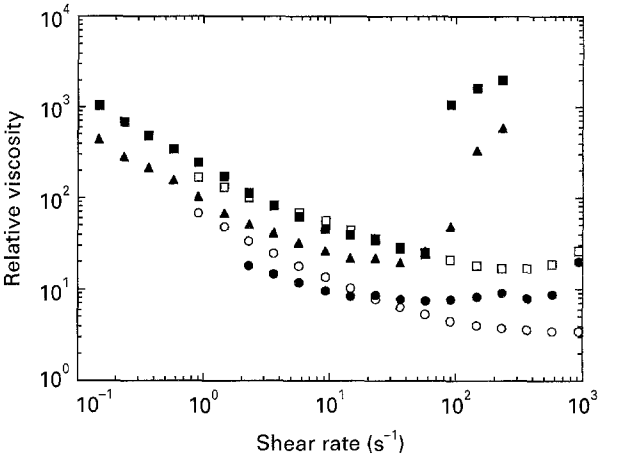

Figure 10 Relative viscosity of silicon carbide whisker suspensions in (●, ▲, ■) aqueous and non-aqueous (○, □) media at different volume fractions of solids: (○) $\phi = 0.109$, (□) $\phi = 0.180$, (●) $\phi = 0.100$, (▲) $\phi = 0.149$, and (■), $\phi = 0.172$.

suspensions are colloidally stable and show an increasing degree of shear thinning with increasing volume fraction of solids. At volume fractions, $\phi < 0.2$, the steady-shear measurements display a Newtonian behaviour with no detectable shear thinning. Measurements on aqueous, colloidally stable alumina suspensions showed a similar behaviour to the non-aqueous suspensions above.

As discussed above, shear thinning of a concentrated colloidally stable suspension can be related to the perturbation of the suspension structure. With the present experimental system it was not possible to attain the limiting low shear region corresponding to the steady-shear response of the undisturbed, relaxed suspension, but the high shear measurements display a plateau corresponding to the steady-shear viscosity of the suspension with a hydrodynamically controlled suspension structure. Hence, it is not possible to define the degree of shear thinning as the relative difference between the low and high shear viscosity limit. Instead, in this context the degree of shear thinning is related to the slope of the steady-shear curve in the low shear-rate region. A high degree of shear thinning corresponds to a large negative slope.

Fig. 9 shows the steady-shear viscosity of non-aqueous silicon carbide whisker suspensions at various volume fractions. These suspensions also display a shear thinning behaviour but compared to the colloidally stable alumina suspensions, the shear thinning is already severe at a volume fraction of solids at $\phi = 0.055$. It was found that non-aqueous suspensions with whisker concentrations as low as $\phi = 0.02$ showed strong shear thinning. The degree of shear thinning of the suspensions at a solids concentration at $\phi = 0.055$ and 0.109 appear to be nearly identical while the degree of shear thinning for the whisker suspension at the highest concentration, $\phi = 0.180$, is substantially lower. A limiting high shear viscosity can be observed, although the most concentrated suspensions seem to display a slightly shear-thickening behaviour. It was difficult to prepare non-aqueous whisker suspensions at solids concentrations higher than $\phi = 0.20$ because the suspensions became almost solid-like at rest and high shear mixing or ultrasonication proved to be almost impossible.

Fig. 10 shows a comparison between the steady-shear relative viscosity of aqueous and non-aqueous silicon carbide whisker suspensions at different

volume fractions. The relative viscosity, η_r, is defined as

$$\eta_r = \eta/\eta_s \quad (5)$$

where η is the suspension viscosity and η_s is the viscosity of the medium. While the non-aqueous, weakly flocculated whisker suspension at the highest concentration shows a continuously shear-thinning behaviour with a tendency of shear thickening at very high shear rates, the aqueous, colloidally stable whisker suspensions display a rather strongly shear-thinning behaviour at low shear rates followed by either continuous or discontinuous shear thickening. The severity of the shear thickening increases with increasing solids concentration. At the highest concentration ($\phi = 0.172$), the aqueous whisker suspension shows a discontinuous shear thickening with a two orders of magnitude increase in viscosity over a narrow shear rate range. Cycling up and down in shear rate did not result in any hysteresis which showed that the shear thickening phenomenon is reversible.

Shear thickening is an important phenomenon which has been extensively studied [45]. Hoffman [37], who was one of the first to investigate shear thickening in detail, attributed the shear thickening to an order–disorder transition of the particle microstructure. Using white light diffraction to probe the suspension structure under shear, he found that the ordered layers which form in the shear-thinning region break up into a less ordered structure at the critical shear rate. This less ordered structure dissipates more energy during flow due to particle "jamming", and hence the viscosity increases. Recent experimental and theoretical studies have tried to elucidate the details of the shear thickening phenomenon. Although there is some debate regarding the mechanisms responsible for shear thickening, most researchers assume that shear thickening only occurs in concentrated suspensions of non-aggregating solid particles [43, 45]. It has been found that the onset of shear thickening is controlled by parameters such as the viscosity of the medium, the particle size and the magnitude of the interparticle repulsion [45–47].

Almost all studies on shear thickening have been performed on monodisperse, spherical particles. However, Boersma *et al.* [47] have shown that the shear-thickening phenomenon becomes less severe when a polydisperse system is used. It was suggested that the effect of polydispersity can be attributed to a modification of the suspension structure and an increase in the maximum volume fraction of solids. It is not expected that a long range order will occur in a polydisperse suspension in the shear thinning region, and hence the order–disorder transition at the onset of shear thickening will be rather weak.

Although it is difficult to find rheological studies on well-characterized rod-like particles in the colloidal size range, there have been several reports on the structure and rheology of larger non-colloidal fibres. Crowson *et al.* [48] studied the fibre orientation in short glass-fibre-filled thermoplastics using glass fibres with diameters of 10 μm and lengths above 500 μm. They found that converging flows resulted in a pronounced fibre alignment along the flow direction, while shear flows had the effect of partially disorienting the fibres, in particular at low shear rates. Clarke [49] found that suspensions of glass rods of a diameter of 30 μm displayed a dilatant, shear-thickening behaviour even at low volume fractions. Hence, these studies show that rod-like fibres can align in a flow field and also display a shear-thickening behaviour.

With this background, it is proposed that the difference in the steady-shear behaviour between the aqueous and non-aqueous whisker suspensions can be related to the difference in colloidal stability. The absence of shear thickening of the non-aqueous whisker suspension is due to the attractive forces between the whiskers, resulting in a flocculated suspension. The severe shear-thickening phenomenon of the aqueous, colloidally stable suspensions can be attributed to an order–disorder transition of the suspension structure at a critical shear rate. The strong shear thinning of the aqueous whisker suspensions indicates that the suspension structure becomes strongly perturbed by shear. It is expected that anisotropic particles such as rod-like whiskers will be strongly affected by flow and change the suspension structure from a random whisker orientation at rest, tending to whisker alignment in the direction of the flow at high shear. This change in suspension structure will result in a high degree of shear thinning. Concurrently, the break up of such a structure with long-range order may explain the observed shear-thickening behaviour.

The silicon carbide whiskers suspended in decalin are weakly flocculated, as discussed in Section 3.1. Hence, the attractive forces between the rod-like whiskers will result in the formation of aggregates. The aggregates formed by attractive interactions between colloidal particles are usually rather heterogeneous with a low average density and thus, tend to immobilize some of the continuous medium (decalin in this case) [39]. The shear thinning of flocculated suspensions can then be related to the continuous breakdown of the aggregates at increasing shear rates. However, the presence of anisotropic, rod-like whiskers and the shear thinning related to whisker alignment complicates the interpretation. It is difficult to distinguish between the effect of breakdown of aggregates and the effect of whisker alignment, because both of these processes will result in a strongly shear-thinning behaviour.

A direct comparison between the relative viscosities of stable and flocculated whisker suspensions suggests that the shear-thinning mechanism of the non-aqueous whisker suspensions depends on the volume fraction (Fig. 10). At low volume fractions ($\phi \sim 0.10$), the non-aqueous suspension appears to have a higher degree of shear thinning than the colloidally stable aqueous suspension. This indicates that the breakdown of aggregates is the dominating mechanism responsible for shear thinning in more dilute flocculated whisker suspensions. However, measurements at lower shear rates are necessary to establish this effect more firmly. Unfortunately, it was not possible to perform such measurements at very low

shear rates due to the very low shear stresses (i.e. low torque readings) in this region.

The comparison of the whisker suspensions at high volume fractions ($\phi \sim 0.18$) shows that the non-aqueous suspension has an identical or possibly lower degree of shear thinning than the colloidally stable, aqueous suspension. A possible explanation of this behaviour is that the suspension structure is perturbed less by shear in the concentrated compared to the more dilute flocculated whisker suspensions. Calculation of the interparticle energy between two rod-like cylinders has shown that a parallel orientation is prefered at rest [29]. Such an orientation maximizes the attractive energy between two cylinders subjected to van der Waals attraction. Hence, it is possible that the concentrated flocculated suspension at rest already has a suspension structure characterized by the whiskers being aligned parallel to each other in aggregated whisker "bundles". The observed shear thinning of the concentrated suspensions can then be attributed to the break-up and alignment of the whisker "bundles". The stronger shear thinning of the more dilute non-aqueous whisker suspensions indicates that the aggregates are more random in orientation at rest. However, direct observations of the suspension structure at rest and during shear are necessary to elucidate the details of this phenomenon.

Fig. 11 shows the steady-shear behaviour of non-aqueous composite suspensions at different total solids concentrations. All the composite suspensions consist of a mixture of 75 wt % Al_2O_3 and 25 wt % SiC_w (equivalent to 30 vol % SiC_w). These suspensions are also characterized by shear thinning with a plateau in the high shear region. The volume fractions range from $\phi = 0.254$–0.405. It was found to be difficult to prepare non-aqueous composite suspensions containing 25 wt % SiC_w at solids concentrations higher than $\phi = 0.42$. Fig. 12 shows the steady-shear behaviour of the aqueous composite suspensions. At intermediate concentrations, shear thinning occurs with an apparent plateau in the high shear region. At high concentrations ($\phi > 0.4$), the suspensions display a shear-thickening behaviour where the severity of the phenomenon increases with increasing concentration.

The rheological behaviour of the composite suspensions can be explained following the detailed characterization of the separate components. The continuous shear thinning of the non-aqueous composite suspensions (Fig. 12) correlates to the continuous shear thinning of the non-aqueous alumina (Fig. 8) and silicon carbide whisker (Fig. 9) suspensions. The shear-thickening behaviour of the concentrated aqueous composite suspensions (Fig. 12) can be explained by the strong shear thickening of the silicon carbide whiskers (Fig. 10).

To the authors' knowledge, shear-thickening behaviour of concentrated composite suspensions has only been reported in one previous study [19]. Tsao *et al.* [19] investigated the rheological behaviour of concentrated Si/SiC_w mixtures suspended in melted polyethylene waxes using capillary viscometry. They found that a concentrated composite suspension (80/20 vol % mixture of silicon powder and SiC

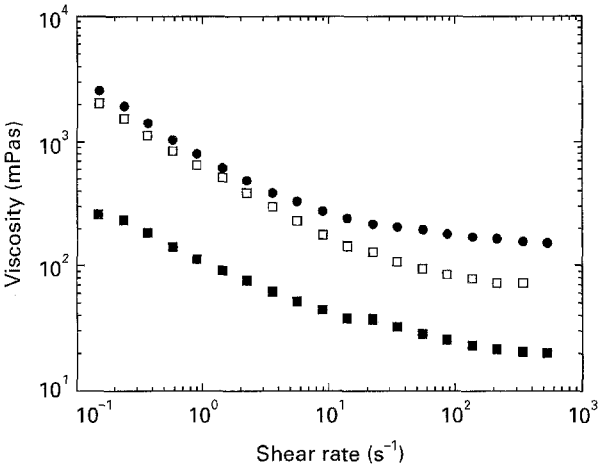

Figure 11 Steady-shear viscosity of composite suspensions containing 75 wt % Al_2O_3 and 25 wt % (30 vol %) SiC_w suspended in decalin with 3.9 wt % Hypermer KD3 at different total volume fraction of solids: ϕ = (■) 0.254, (□) 0.355, (●) 0.405.

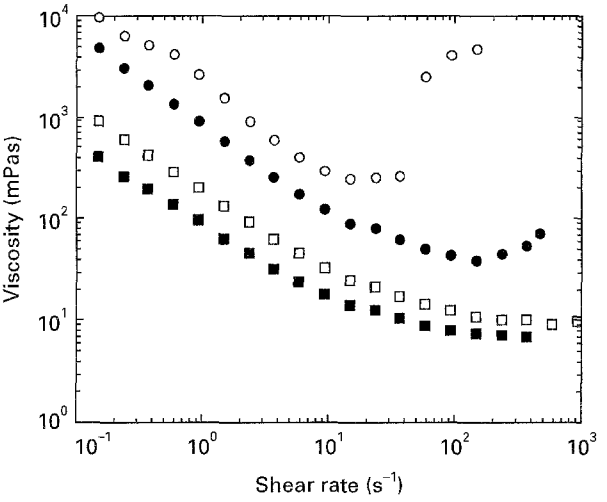

Figure 12 Steady-shear viscosity of aqueous composite suspensions containing 25 wt % (30 vol %) SiC_w dispersed at pH ~ 9 with 0.25 wt % Dispex A40 added. Measurements were performed on different total volume fractions of solids: ϕ = (■) 0.25, (□) 0.30, (●) 0.40, (○) 0.43.

whisker) at $\phi = 0.60$ total solids concentration, displayed a shear-thickening behaviour at high shear rates. However, the shear-thickening effect was rather weak with an increase in viscosity of only ~25% and it was necessary to perform a large wall-slip correction to obtain these results. Stedman *et al.* [18] investigated the behaviour of Si_3N_4/SiC_w composite suspensions suspended in mixtures of polypropylene, microcrystalline wax and stearic acid using capillary viscometry. Their results showed that both the Si_3N_4 suspensions, as well as the composite mixtures, displayed a continuously shear-thinning behaviour. However, no correction or control of wall slip was reported in their study.

Viscosity measurements on aqueous Si_3N_4/SiC_w [11] and Al_2O_3/SiC_w [13] composite suspensions have shown a rather weakly shear-thinning behaviour with no evidence of shear thickening. Hence, none of these previous studies has shown such a strong

shear-thickening phenomenon as displayed by the present aqueous composite suspension at the highest concentration (Fig. 12). Because many suspension parameters, e.g. particle-size distribution, whisker aspect ratio, whisker concentration, colloidal stability of the suspension, as well as measurement details, for example type of rheological equipment, shear-rate range investigated, will affect the observed rheological behaviour, it is difficult to compare directly the present results with these reported studies. The systems studied, the whisker source as well as the rheological methods used, varied between the different studies. However, from the comparison between the stable and flocculated suspensions in the present study, it is believed that the colloidal stability of the suspension is the most important parameter.

The direct comparison between the aqueous and non-aqueous composite suspensions (Fig. 13) shows some interesting features. The degree of shear thinning is substantially smaller for the non-aqueous composite suspension. This effect can be related to the discussion above, regarding the shear thinning of the non-aqueous flocculated silicon carbide whisker suspensions. The low degree of shear thinning indicates that the rod-like whisker already at rest has obtained a parallel alignment, possibly in the form of small whisker "bundles". The aqueous composite suspensions containing colloidally stable whiskers show a high degree of shear thinning which indicates a strong perturbation of the suspension structure by shear. Comparision of the aqueous and non-aqueous composite suspensions at $\phi = 0.25$ shows that the curves coincide at high shear rates and finally yield an identical high shear viscosity plateau. This indicates that the suspension structure is similar in the two suspensions at high shear, suggesting that the whisker aggregates present in the non-aqueous composite suspensions have been broken up into the separate whiskers. The comparison between the highly concentrated composite suspensions is complicated by the shear thickening phenomenon displayed by the aqueous composite suspensions.

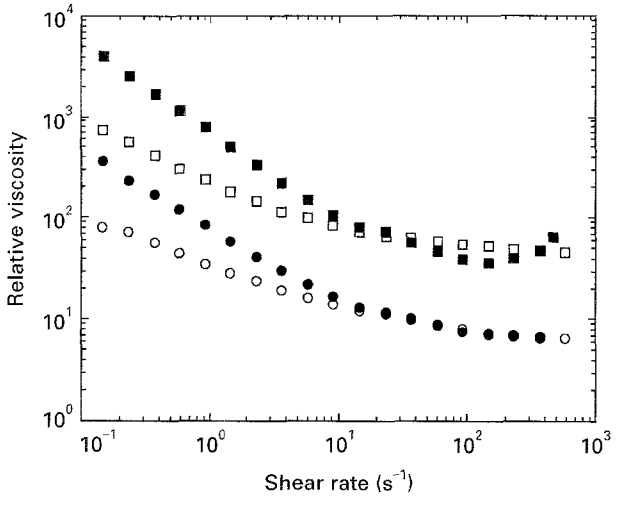

Figure 13 Relative viscosity of composite suspensions containing 25 wt % (30 vol %) SiC_w in aqueous (●, ■) and non-aqueous (○, □) media at different total volume fractions of solids. $\phi = (○, ●)$ 0.25, (□, ■) 0.40.

The comparison between aqueous and non-aqueous silicon carbide whisker suspensions (Fig. 10) showed a similar type of behaviour. At high volume fractions ($\phi \sim 0.18$), the two curves almost coincide at shear rates below the onset of shear thickening, indicating that the whisker aggregates present in the non-aqueous suspensions are broken down at high shear rates.

3.4. Volume-fraction dependence of the viscosity

The viscosity of concentrated suspensions depend strongly on the volume fraction of the solid phase. Although attempts have been made to include many-body interactions into theoretical calculations of the relative viscosity of concentrated hard-sphere suspensions [50, 51], different types of phenomenalistic or semi-empirical models are commonly used to fit experimental data.

Hard sphere and near hard sphere suspensions [52, 53] have been successfully described by using the Krieger–Dougherty model [54]

$$\eta_r = (1 - \phi/\phi_m)^{-[\eta]\phi_m} \quad (6)$$

where $[\eta]$ is the intrinsic viscosity, or the Quemada model [55]

$$\eta_r = (1 - \phi/\phi_m)^{-2} \quad (7)$$

Chong *et al.*'s equation [56]

$$\eta_r = [1 + (0.75\phi/\phi_m)/(1 - \phi/\phi_m)]^2 \quad (8)$$

has been used to fit rheological data of both silicon nitride and composite suspensions [18]. All of these expressions have in common that they include the maximum volume fraction, ϕ_m, to account for the approach to infinite viscosity (solid body) at some critical volume fraction of solids. Equations 7 and 8 only have ϕ_m as a parameter, while Equation 6 also has $[\eta]$ as a parameter. The intrinsic viscosity relates to the effect on the relative viscosity of non-interacting particles in very dilute suspensions. $[\eta]$ is 2.5 for spheres and expected to increase with increasing anisotropy of the solid phase.

Fig. 14 shows the volume fraction dependence of the relative viscosity of the non-aqueous alumina and silicon carbide whisker suspensions. The experimental points in Fig. 14 were fitted to a modified Krieger–Dougerty equation

$$\eta_r = (1 - \phi/\phi_m)^{-n} \quad (9)$$

where ϕ_m and n are used as fitting parameters (Table III). It was considered incorrect to use $[\eta]$ as an independent fitting parameter in the original Krieger–Dougherty equation. It was not possible to obtain a satisfactorily fit of the experimental data to either the Quemada or the Chong equation. Both of these expressions predict a much more abrupt increase in relative viscosity with volume fraction than was experimentally observed as illustrated in Fig. 14. Hence, it is considered necessary to use a two-parameter equation to be able to describe the general η_r–ϕ relation of technical suspensions. Zhang and Evans

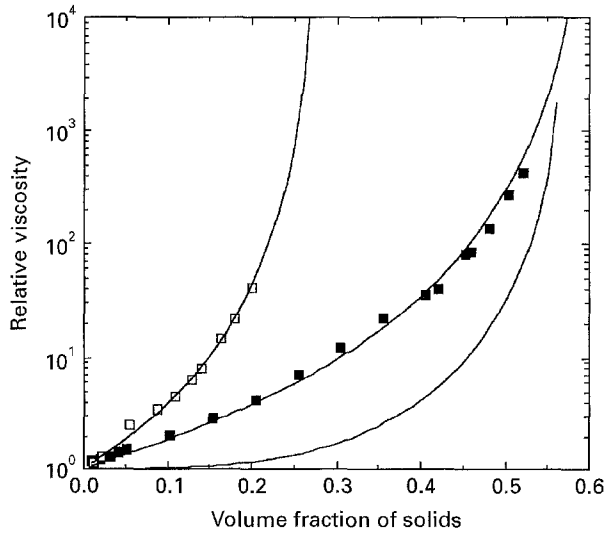

Figure 14 Relative viscosity as a function of volume fraction of solids for non-aqueous suspensions. The viscosities correspond to the high shear plateau. (□) SiC_w in decalin, (■) Al_2O_3 in decalin. The experimental points were fitted to the modified Krieger–Dougherty equation. (—) The predicted relative viscosity function according to Chong *et al.*'s equation using $\phi_m = 0.57$.

TABLE III Best fitting parameters to the η_r–ϕ results shown in Fig. 15 by using the modified Krieger–Dougerty equation

Material	Solvent	ϕ_m	n
Al_2O_3	Decalin	0.61	3.3
SiC_w	Decalin	0.28	3.0

[57] made Chong *et al.*'s equation (Equation 8) more general by recasting it into a two-parameter relation

$$\eta_r = [(\phi_m - C\phi)/(\phi_m - \phi)]^2 \qquad (10)$$

to accommodate many types of concentrated ceramic suspension. This equation, with C and ϕ_m as independent fitting parameters, could probably have been used as well as Equation 9 above to fit the experimental data. The best fit of the experimental data to Equation 9 shows that the maximum volume fraction is drastically lower for the SiC_w suspension ($\phi_m = 0.28$) compared to the alumina suspension ($\phi_m = 0.61$). This low maximum volume fraction of the SiC whisker suspensions agree with previous studies. Experimental studies have shown that the maximum packing volume fraction of rods decreases rapidly with increasing aspect ratio [58].

Earlier studies on hard sphere suspensions have obtained $\phi_m = 0.71$ in the high shear limit [52, 53], hence substantially higher than the observed value for the non-aqueous alumina suspensions. This difference can be explained by the volume taken by the dispersant KD3. Using the concept of effective volume fraction, ϕ_{eff}, discussed in Section 3.2, it is possible to accommodate for some of this effect. Calculation of the effective volume fraction of an alumina suspension with 4.5 wt % KD3 added using Equation 3 shows that $\phi = 0.61$ (solids) corresponds to $\phi_{eff} = 0.73$. In fact, this is probably an underestimation of the effective volume fraction because it is assumed that the surrounding polymer layer is completely dense. Probably, the polymer layer density is lower with some decalin being dissolved in the layer, thus increasing the volume of the polymer layer. With the alumina powder having a rather broad particle-size distribution it is expected that the maximum effective volume fraction should be larger than the value for monodisperse particles. Several studies have shown how the use of bimodal or continuous broad particle-size distributions can lower the viscosity and increase the maximum volume fraction [56, 59, 60].

Farris [61] was one of the first to attempt to describe theoretically the viscosity of multimodal suspensions of rigid particles. He developed a model in which the viscosity of multimodal suspensions was determined from the viscosity–concentration behaviour of the unimodal components. His model is based on the assumption that the large component is large enough so that the small components can be viewed as a continuum. Using a bimodal mixture of monodisperse spheres, this restriction relates to a size ratio, $d_{large}/d_{small} > 10$, where d is the diameter of the particle. Fig. 15 shows the experimental results of the non-aqueous composite suspensions being fitted to the Farris model [61]. The results from some of the aqueous composite suspensions are also included, in case a high shear plateau could be identified. It was found that the Farris theory can describe the experimental results quite successfully. This is a somewhat surprising result considering the size difference between the whiskers and the particles and the rod-like shape of the whiskers. The Farris theory was originally developed for multimodal mixtures of monodisperse spheres, but the results in Fig. 15 shows that it can also be applied to mixtures of non-spherical particles. This result also indicates that it is sufficient if the coarse component has one dimension which is > 10 times larger than the fine component. The average length of the whiskers is approximately 10 times larger than the average diameter of the alumina particles while the whisker diameter roughly equals the particle diameter.

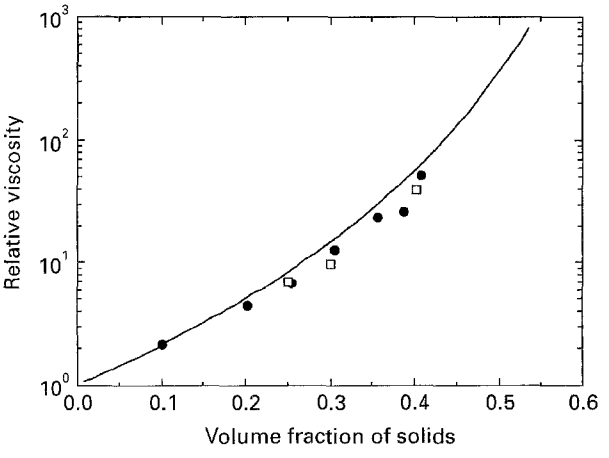

Figure 15 Relative viscosity as a function of volume fraction of solids for Al_2O_3/25 wt % SiC_w composite suspensions in (●) decalin, and (□) aqueous media. The viscosities correspond to the high shear plateau. The continuous line corresponds to the predicted viscosities using the Farris theory.

However, more experiments where the whisker content is varied are needed to establish the applicability of the Farris theory more firmly. The present results may be fortuitous because the η_r–ϕ relation for the composite suspension is rather similar to the results for the alumina suspension. Hence, the studied whisker addition (30 vol %) does not seem to affect the relative viscosity to a great extent. A stronger increase in relative viscosity is expected at higher whisker fractions.

4. Conclusion

Rheological characterization of concentrated suspensions containing alumina particles, silicon carbide whiskers and mixtures thereof, have been performed and the behaviour has been discussed in relation to the particle interactions and the suspension structure. The colloidal stability of alumina particle and silicon carbide whisker suspensions in both aqueous and non-aqueous media has been characterized. The aqueous suspensions, stabilized with the addition of an anionic polyelectrolyte, were colloidally stable. The silicon carbide whisker non-aqueous suspension, sterically stabilized with the addition of a polymeric dispersant in decalin, was flocculated, while the non-aqueous alumina suspension was colloidally stable. It was demonstrated how rheological measurements can be used to optimize the amount of dispersant added. By combining steady-shear measurements at both high and low shear rates and viscoelastic measurements, it was possible to minimize the amount of added dispersant while maintaining the colloidal stability.

The steady-shear rheological behaviour was thoroughly characterized. It was found that all the concentrated suspensions displayed a more or less severe shear-thinning behaviour with a high shear plateau. The concentrated aqueous SiC_w and composite suspensions showed a strong, sometimes discontinuous, shear thickening at some critical shear rate. This behaviour was attributed to a possible order–disorder transition of the suspension structure. Colloidal stability of the whiskers is a condition for shear thickening to occur, because no shear-thickening behaviour could be detected for the non-aqueous SiC_w and the composite suspensions.

It was possible to fit the volume fraction dependence of both the SiC_w as well as the alumina suspensions to a modified Krieger–Dougherty model. The obtained maximum volume fractions where flow ceases were rather low for the whiskers ($\phi_m = 0.28$), illustrating the poor packing of rods. The viscosity of the composite suspensions was successfully predicted from the Farris theory using the rheological data for the separate components. With the use of the Farris theory, it should be possible to predict the effect of the volume fraction of whiskers and the whisker aspect ratio on the viscosity and the maximum packing density of composite suspensions.

Acknowledgements

The Swedish National Board for Industrial and Technical Development and Sandvik Coromant AB are thanked for financial support. The author thanks Eva Sjöström for performing most of the rheological measurements, Eva Liden and Brita Nyberg, Swedish Ceramic Institute, for fruitful discussions and for performing the particle-size measurements, and Marianne Collin, Sandvik Coromant, for providing and characterizing the alumina powder and the silicon carbide whiskers.

References

1. A. A. GRIFFITH, *Phil. Trans. R. Soc. Lond.* **A221** (1920) 163.
2. F. F. LANGE, *J. Am. Ceram. Soc.* **72** (1989) 3.
3. I. A. AKSAY, in "Advances in Ceramics", Vol. 9, edited by J. A. Mangels and G. L. Messing (American Ceramic Society, Columbus, OH, 1984) p. 94.
4. R. J. PUGH and L. BERGSTRÖM (eds), "Surface and Colloid Chemistry in Advanced Ceramics Processing" (Marcel Dekker, New York, 1994).
5. P. F. BECHER, *J. Am. Ceram. Soc.* **74** (1991) 255.
6. T. N. TIEGS and P. F. BECHER, *Am. Ceram. Soc. Bull.* **66** (1987) 339.
7. J. R. PORTER, F. F. LANGE and A. H. CHOKSHI, *ibid.* **66** (1987) 343.
8. P. D. SHALEK, J. J. PETROVIC, G. F. HURLEY and F. D. GAC, *ibid.* **65** (1986) 338.
9. P. F. BECHER and G. C. WEI, *J. Am. Ceram. Soc.* **67** (1984) C-267.
10. R. LUNDBERG, B. NYBERG, K. WILLIANDER, M. PERSSON and R. CARLSSON, *Composites* **18** (1987) 125.
11. M. J. HOFFMANN, A. NAGEL, P. GREIL and G. PETZOW, *J. Am. Ceram. Soc.* **72** (1989) 765.
12. Y. HIRATA, S. MATSUSHITA, S. NAKAGAMA, Y. ISHIHARA and S. HORI, *J. Ceram. Soc. Jpn.* **97** (1989) 881.
13. M. D. SACKS, H.-W. LEE and O. E. ROJAS, *J. Am. Ceram. Soc.* **71** (1988) 370.
14. I. TSAO and S. C. DANFORTH, *Bull. Am. Ceram. Soc.* **72** (1993) 55.
15. L. BERGSTRÖM, in "Surface and Colloid Chemistry in Advanced Ceramics Processing", edited by R. J. Pugh and L. Bergström (Marcel Dekker, New York 1994) p. 193.
16. W. B. RUSELL, D. A. SAVILLE and W. R. SCHOWALTER, "Colloidal Dispersions" (Cambridge University Press, Cambridge 1989) Ch. 14.
17. T. KITANO, T. KATAOKA and T. SHIROTA, *Rheol. Acta* **20** (1981) 207.
18. S. J. STEDMAN, J. R. G. EVANS and J. WOODTHORPE, *J. Mater. Sci.* **25** (1990) 1833.
19. I. TSAO, S. C. DANFORTH and A. B. METZNER, *J. Am. Ceram. Soc.* **76** (1993) 2977.
20. B. J. WRONA, J. F. RHODES and W. M. ROGERS, in "Proceedings of the 16th Annual Conference on Composites and Advanced Ceramic Materials", Cocoa Beach 1992, edited by M. I. Mendelson (American Ceramic Society, Westerville, OH, 1992) p. 653.
21. T. N. TIEGS and D. M. DILLARD, *J. Am. Ceram. Soc.* **73** (1990) 1440.
22. "*Cis- and Trans-Decalin*", API Monograph Series, API Publication 706, October 1978.
23. J. D. SCHOFIELD, private communication (1990).
24. G. MARIN, in "Rheological Measurements", edited by A. A. Collyer and D. W. Clegg (Elsevier, London, 1988) p. 297.
25. M. ROBINSON, J. A. PARK and D. W. FUERSTENAU, *J. Am. Ceram. Soc.* **47** (1964) 516.
26. D. BALLION and N. JAGGRREZIC-RENAULT, *J. Radio-Analyt. Nucl. Chem.* **92** (1985) 133.
27. M. J. CRIMP, R. E. JOHNSON Jr, J. W. HALLORAN and D. L. FEKE, in "Science of Ceramic Chemical Processing", edited by L. L. Hench and D. R. Ulrich (Wiley, New York, 1986) p. 539.
28. R. J. PUGH and L. BERGSTRÖM, *J. Coll. Interface Sci.* **124** (1988) 570.
29. L. BERGSTRÖM, in preparation.

30. O. LYCKFELDT, E. BOSTEDT, M. PERSSON, R. CARLSSON and L. BERGSTRÖM, in "Ceramics Today-Tomorrows Ceramics", edited by P. Vinzenzini (Elsevier, Amsterdam, 1991) p. 1005.
31. L. BERGSTRÖM and O. LYCKFELDT, in "Structural Ceramics- Processing, Microstructure and Properties", edited by J. J. Bentzen, J. B. Bilde-Sørensen, N. Christiansen, A. Horsewell and B. Ralph (Risö National Laboratory, Roskilde, Denmark, 1990) p. 193.
32. J. CESARANO III, I. A. AKSAY and A. BLEIER, *J. Am. Ceram. Soc.* **71** (1988) 250.
33. R. J. PUGH, in "Surface and Colloid Chemistry in Advanced Ceramics Processing", edited by R. J. Pugh and L. Bergström (Marcel Dekker, New York, 1994) p. 127.
34. D. H. NAPPER, "Polymeric Stabilization of Colloidal Dispersions" (Academic Press, London, 1982).
35. Th. F. TADROS (ed.) "The Effect of Polymers on Dispersion Properties" (Academic press, London, 1982).
36. C. G. de KRUIF, in "Hydrodynamics of Dispersed Media", edited by J. P. Hulin, A. M. Cazabat, E. Guyon and F. Carmona (Elsevier, North Holland, 1990) p. 79.
37. R. L. HOFFMAN, *Trans. Soc. Rheol.* **16** (1972) 155.
38. B. J. ACKERSON and N. A. CLARK, *Physica* **118A** (1983) 221.
39. R. J. HUNTER, *Adv. Coll. Interface Sci.* **17** (1982) 197.
40. A. T. J. M. WOUTERSEN and C. G. de KRUIF, *J. Chem. Phys.* **94** (1991) 5739.
41. R. BUSCALL, P. D. A. MILLS and G. E. YATES, *Coll. Surf.* **18** (1986) 341.
42. M. CHEN and W. B. RUSSEL, *J. Coll. Interface Sci.* **141** (1991) 564.
43. G. N. CHOI and I. M. KRIEGER, *ibid.* **113** (1986) 101.
44. D. A. R. JONES, B. LEARY and D. V. BOGER, *ibid.* **150** (1992) 84.
45. H. A. BARNES, *J. Rheol.* **33** (1989) 329.
46. R. L. HOFFMAN, *J. Coll. Interface Sci.* **46** (1974) 491.
47. W. H. BOERSMA, J. LAVEN and H. N. STEIN, *AIChEJ.* **36** (1990) 321.
48. R. J. CROWSON, M. J. FOLKES and P. F. BRIGHT, *Polym. Eng. Sci.* **20** (1980) 925.
49. B. CLARKE, *Trans. Inst. Chem. Eng.* **45** (1967) 251.
50. C. W. J. BEENAKKER, *Physica A* **128** (1984) 48.
51. W. B. RUSSEL and A. P. GAST, *J. Chem. Phys.* **84** (1986) 1815.
52. J. C. van der WERFF and C. G. de KRUIF, *J. Rheol.* **33** (1989).
53. D. A. R. JONES, B. LEARY and D. BOGER, *J. Coll. Interface Sci.* **147** (1991) 479.
54. I. M. KRIEGER and T. J. DOUGHERTY, *Trans. Soc. Rheol.* **3** (1959) 137.
55. D. E. QUEMADA, in "Lecture Notes in Physics, Stability of Thermodynamic Systems", edited by J. Cases-Vasquez and J. Lebon (Springer, Berlin, 1982) p. 210.
56. J. S. CHONG, E. B. CHRISTIANSEN and A. D. BEAR, *J. Appl. Polym. Sci.* **15** (1971) 2007.
57. T. ZHANG and J. R. G. EVANS, *J. Eur. Ceram. Soc.* **5** (1989) 165.
58. J. V. MILEWSKI, *Adv. Ceram. Mater.* **1** (1986) 36.
59. D. I. LEE, *J. Paint Technol.* **42** (1970) 579.
60. S. C. TSAI, D. BOTTS and J. PLOUFF, *J. Rheol.* **36** (1992) 1291.
61. R. J. FARRIS, *Trans. Soc. Rheol.* **12** (1968) 281.

Received 27 May 1994
and accepted 22 March 1995